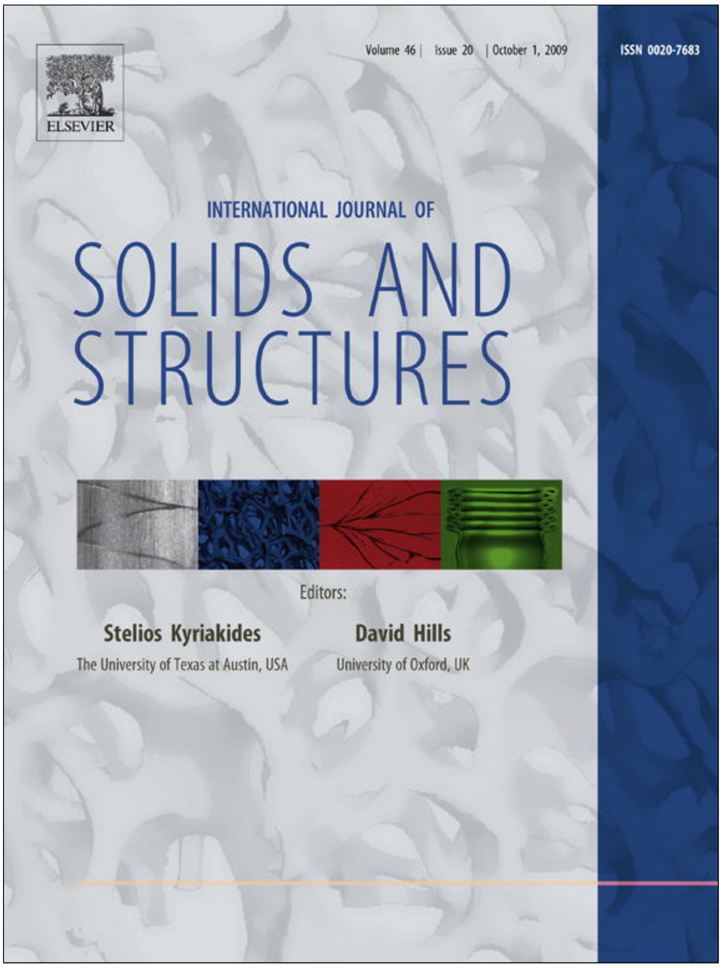
Volume 46 | Issue 20 | October 1, 2009
ISSN 0020-7683
ELSEVIER
INTERNATIONAL JOURNAL OF
SOLIDS AND STRUCTURES
Editors:
Stelios Kyriakides
The University of Texas at Austin, USA
David Hills
University of Oxford, UK

International Journal of Solids and Structures 46 (2009) 3664–3668

Contents lists available at ScienceDirect

International Journal of Solids and Structures

journal homepage: www.elsevier.com/locate/ijsolstr

Repetitive beam-like structures: Distributed loading and intermediate support

N.G. Stephen *

School of Engineering Sciences, Mechanical Engineering, University of Southampton, Highfield, Southampton SO17 1BJ, UK

ARTICLE INFO

Article history:
Received 15 July 2008
Available online 24 June 2009

Keywords:
Repetitive structure
Transfer matrix
Jordan canonical form
Participation coefficients

ABSTRACT

Theory is developed for the elastostatic transfer matrix analysis of a repetitive beam-like structure subject to point-wise distributed loading, with and without an intermediate support; this complements previous work in which loading is applied at one end only and reacted at the other. State-vectors are expressed in terms of participation coefficients of the eigen- and principal vectors, leading to the simplest description of the evolution of nodal displacement and force components as one moves along the structure, in terms of powers of the Jordan canonical form. Inaccuracy due to ill-conditioning is explained in terms of powers of greater than unity eigenvalues.

1. Introduction

Repetitive (or periodic) structures are analysed very efficiently when such periodicity is taken into account; in general, the behaviour of a complete structure can be determined through the analysis of a single repeating cell, together with boundary conditions if the structure is not of infinite extent. A typical approach, (Langley, 1996), relates a state-vector of displacement and force components on either side of a generic repeating cell by a transfer matrix $\mathbf{G}$. The stiffness matrix $\mathbf{K}$ of the single cell relates the force and displacement vectors on both sides as $\mathbf{F} = \mathbf{Kd}$, or in partitioned form

$$\begin{bmatrix} \mathbf{F}_L \\ \mathbf{F}_R \end{bmatrix} = \begin{bmatrix} \mathbf{K}_{LL} & \mathbf{K}_{LR} \\ \mathbf{K}_{RL} & \mathbf{K}_{RR} \end{bmatrix} \begin{bmatrix} \mathbf{d}_L \\ \mathbf{d}_R \end{bmatrix}, \tag{1}$$

where the subscripts L and R denote left and right, respectively. The transfer matrix $\mathbf{G}$ is determined from the stiffness matrix $\mathbf{K}$ according to

$$\begin{bmatrix} \mathbf{d}_R \\ \mathbf{F}_R \end{bmatrix} = \begin{bmatrix} -\mathbf{K}_{LR}^{-1}\mathbf{K}_{LL} & -\mathbf{K}_{LR}^{-1} \\ \mathbf{K}_{RL} - \mathbf{K}_{RR}\mathbf{K}_{LR}^{-1}\mathbf{K}_{LL} & -\mathbf{K}_{RR}\mathbf{K}_{LR}^{-1} \end{bmatrix} \begin{bmatrix} \mathbf{d}_L \\ -\mathbf{F}_L \end{bmatrix}, \tag{2}$$

or more compactly $\mathbf{s}_R = \mathbf{G}\mathbf{s}_L$; the transfer matrix $\mathbf{G}$ and state-vectors $\mathbf{s}$ are defined accordingly. While transfer matrix analysis typically employs the sign conventions of the theory of elasticity, here it is more convenient to employ the force sign conventions of finite element analysis (FEA), hence the negative force vector on the right-hand side of Eq. (2). The transfer matrix thus describes how a state-vector evolves as one moves from one cell to the next.

Now, an eigenvector of the transfer matrix $\mathbf{G}$ represents a pattern of nodal displacement and force components, which is unique to within a scalar multiplier, say λ. Translational symmetry demands that this pattern is preserved as one moves from cell-to-cell, implying that $\mathbf{s}_R = \lambda\mathbf{s}_L$, which leads directly to the standard eigenproblem

$$(\mathbf{G} - \lambda\mathbf{I})\mathbf{s}_L = \mathbf{0}. \tag{3}$$

Non-unity eigenvalues of $\mathbf{G}$ are the rates of decay of self-equilibrated loading, as anticipated by Saint-Venant's principle. Multiple unity eigenvalues pertain to the transmission of load, e.g. tension, or bending moment, as well as the rigid-body displacements and rotations. Equivalent (homogenized) continuum properties, such as cross-sectional area, second moment of area and Poisson's ratio, can also be determined from the associated eigen- and principal vectors. This transfer matrix approach has been applied to the elastostatic analysis of prismatic (Stephen and Wang, 1996), curved (Stephen and Ghosh, 2005) and pre-twisted (Stephen and Zhang, 2006) repetitive beam-like structures, and a variety of general results pertaining to transfer matrices has been presented in (Stephen, 2006); this includes use of the Moore–Penrose pseudoinverse as a rational method of calculating the principal vectors.

However in all of the examples considered above, it was assumed that loading is applied at one end of the structure only, and reacted at the other. The primary objective of the present paper is to develop the necessary theory for repetitive structures subject to (point-wise) distributed loading, including the effect of an intermediate support. A secondary objective is to present the theory in terms of the participation coefficients of the eigen- and principal vectors, which is surely the simplest possible expression of the spatial evolution, in terms of powers of the Jordan canonical form. Moreover, inaccuracy due to ill-conditioning is readily explained in terms of powers of greater than unity eigenvalues.

The treated structure is shown in Fig. 1, and consists of pin-jointed rods or struts with properties: Young's modulus

* Tel.: +44 0 23 80592359; fax: +44 0 23 80593230.
E-mail address: ngs@soton.ac.uk

0020-7683/$ - see front matter © 2009 Elsevier Ltd. All rights reserved.
doi:10.1016/j.ijsolstr.2009.06.016

Nomenclature

A	cross-sectional area	l, L	length of cell, beam
$\mathbf{C}$, C	vector of, participation coefficient	n, r	index
$\mathbf{d}$	displacement vector	$\mathbf{s}$	state-vector
E	Young's modulus	$\mathbf{T}$	transformation matrix of eigen- and principal vectors
$\mathbf{F}$, F	force vector, component	u, v	displacement components in x- and y-directions
$\mathbf{G}$	transfer matrix	x, y	planar Cartesian coordinates
$\mathbf{I}$	identity matrix	$\mathbf{X}$	eigen- or principal vector
$\mathbf{J}$	Jordan canonical form	λ	eigenvalue
$\mathbf{K}$	stiffness matrix		

$E = 200$ GPa, horizontal and vertical rods of length $l = 1$ m and cross-sectional area 1 cm^2, diagonal rods of length $\sqrt{2}$ m and cross-sectional area 1/2 cm^2; the eigenanalysis of the single cell is described fully by Stephen and Wang (1996). The distributed loading consists of forces of 1 kN applied at each of ten nodal cross-sections. Theory is developed largely in respect of this specific example, but generalisation to other repetitive structures is straightforward.

Finally, note that the transfer matrix method (TMM) calculations were performed using MATLAB, including a symbolic computation toolkit, to double precision; the benchmark FEA was performed using ANSYS.

2. Theory development

While the notation employed in the Introduction is adequate for the eigenanalysis of just a single cell, the inclusion of external loading at the nodal cross-sections requires a more detailed notation. Consider the nth and the $(n+1)$th cells, as shown in Fig. 2. For the nth cell one has

$$\begin{bmatrix} \mathbf{d}(n) \\ \mathbf{F}(n) \end{bmatrix}^n = \begin{bmatrix} \mathbf{G}_{dd} & \mathbf{G}_{dF} \\ \mathbf{G}_{Fd} & \mathbf{G}_{FF} \end{bmatrix} \begin{bmatrix} \mathbf{d}(n-1) \\ -\mathbf{F}(n-1) \end{bmatrix}^n, \tag{4}$$

while for the $(n+1)$th, one has

$$\begin{bmatrix} \mathbf{d}(n+1) \\ \mathbf{F}(n+1) \end{bmatrix}^{n+1} = \begin{bmatrix} \mathbf{G}_{dd} & \mathbf{G}_{dF} \\ \mathbf{G}_{Fd} & \mathbf{G}_{FF} \end{bmatrix} \begin{bmatrix} \mathbf{d}(n) \\ -\mathbf{F}(n) \end{bmatrix}^{n+1}; \tag{5}$$

in the above, the superscript pertains to the cell, the argument denotes the nodal cross-section, and the transfer matrix $\mathbf{G}$ is written in partitioned form. Compatibility of displacement at the nth nodal cross-section, requires

$$\mathbf{d}(n)^n = \mathbf{d}(n)^{n+1}, \tag{6}$$

and in the absence of external loads, force equilibrium requires

$$\mathbf{F}(n)^n + \mathbf{F}(n)^{n+1} = \mathbf{0}. \tag{7}$$

Substitution of Eqs. (6) and (7) into Eq. (5) gives

$$\begin{bmatrix} \mathbf{d}(n+1) \\ \mathbf{F}(n+1) \end{bmatrix}^{n+1} = \begin{bmatrix} \mathbf{G}_{dd} & \mathbf{G}_{dF} \\ \mathbf{G}_{Fd} & \mathbf{G}_{FF} \end{bmatrix} \begin{bmatrix} \mathbf{d}(n) \\ \mathbf{F}(n) \end{bmatrix}^{n}, \tag{8}$$

or more compactly

$$\mathbf{s}(n+1) = \mathbf{G}\mathbf{s}(n). \tag{9}$$

Eq. (9) relates the state-vector on the right-hand side of the $(n+1)$th cell to the state-vector on the right-hand side of the nth cell.

Now suppose that an external force vector $\mathbf{F}_{ext}(n)$ is applied at the nth nodal cross-section; the requirement of displacement compatibility, Eq. (6) is unchanged while force equilibrium, Fig. 2, now requires

$$\mathbf{F}(n)^n + \mathbf{F}(n)^{n+1} = \mathbf{F}_{ext}(n). \tag{10}$$

Substitution of Eqs. (6) and (10) into Eq. (5) gives

$$\begin{bmatrix} \mathbf{d}(n+1) \\ \mathbf{F}(n+1) \end{bmatrix}^{n+1} = \begin{bmatrix} \mathbf{G}_{dd} & \mathbf{G}_{dF} \\ \mathbf{G}_{Fd} & \mathbf{G}_{FF} \end{bmatrix} \begin{bmatrix} \mathbf{d}(n) \\ \mathbf{F}(n) - \mathbf{F}_{ext}(n) \end{bmatrix}^{n}, \tag{11}$$

or more compactly

$$\mathbf{s}(n+1) = \mathbf{G}\mathbf{s}(n) - \mathbf{G}\begin{bmatrix} \mathbf{0} \\ \mathbf{F}_{ext}(n) \end{bmatrix}. \tag{12}$$

Suppose that external forces are applied at the 1st, 2nd, 3rd etc., nodal cross-sections; the state-vectors are then calculated as

$$\mathbf{s}(1) = \mathbf{G}\mathbf{s}(0), \tag{13}$$

$$\mathbf{s}(2) = \mathbf{G}\mathbf{s}(1) - \mathbf{G}\begin{bmatrix} \mathbf{0} \\ \mathbf{F}_{ext}(1) \end{bmatrix} = \mathbf{G}^2\mathbf{s}(0) - \mathbf{G}\begin{bmatrix} \mathbf{0} \\ \mathbf{F}_{ext}(1) \end{bmatrix}, \tag{14}$$

$$\mathbf{s}(3) = \mathbf{G}\mathbf{s}(2) - \mathbf{G}\begin{bmatrix} \mathbf{0} \\ \mathbf{F}_{ext}(2) \end{bmatrix} = \mathbf{G}^3\mathbf{s}(0) - \mathbf{G}^2\begin{bmatrix} \mathbf{0} \\ \mathbf{F}_{ext}(1) \end{bmatrix} - \mathbf{G}\begin{bmatrix} \mathbf{0} \\ \mathbf{F}_{ext}(2) \end{bmatrix}, \tag{15}$$

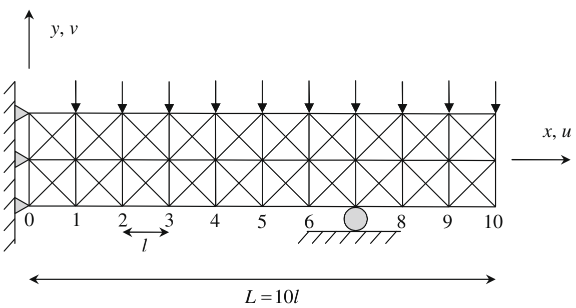

Fig. 1. Ten-cell repetitive structure subject to distributed loading, with an intermediate support at the 7th nodal cross-section. Each downward arrow represents a force of 1 kN.

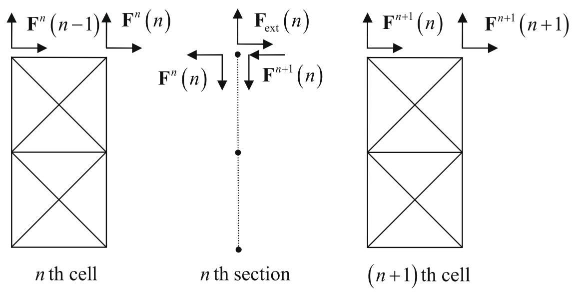

Fig. 2. The nth and $(n+1)$th cells, together with force vectors applied to the nth cross-section; for clarity these are shown on the uppermost nodes only. The superscript and argument pertain to the cell and cross-section, respectively.

$$\mathbf{s}(4) = \mathbf{Gs}(3) + \mathbf{G}\begin{bmatrix}\mathbf{0}\\ \mathbf{F}_{\text{ext}}(3)\end{bmatrix} = \mathbf{G}^4\mathbf{s}(0) - \mathbf{G}^3\begin{bmatrix}\mathbf{0}\\ \mathbf{F}_{\text{ext}}(1)\end{bmatrix} - \mathbf{G}^2\begin{bmatrix}\mathbf{0}\\ \mathbf{F}_{\text{ext}}(2)\end{bmatrix} - \mathbf{G}\begin{bmatrix}\mathbf{0}\\ \mathbf{F}_{\text{ext}}(3)\end{bmatrix}, \tag{16}$$

and the general expression is

$$\mathbf{s}(n) = \mathbf{G}^n\mathbf{s}(0) - \sum_{r=1}^{n-1}\mathbf{G}^{n-r}\begin{bmatrix}\mathbf{0}\\ \mathbf{F}_{\text{ext}}(r)\end{bmatrix}; \tag{17}$$

note that the superscript now denotes powers of the transfer matrix.

Although Eq. (17) lies at the heart of the present analysis, it cannot be applied directly, as the state-vector $\mathbf{s}(0)$ is not yet completely known. For the example shown in Fig. 1, one has incomplete knowledge of the state-vector at the two ends: the applied force vector on the right-hand end $\mathbf{F}(10)$ is known, but the free-end displacement vector $\mathbf{d}$ (10) is not. At the fully fixed left-hand end, the vector $\mathbf{d}(0)$ is known (equal to a column vector of zeros) while the reaction vector $\mathbf{F}(0)$ is not.

3. Participation coefficients

The expansion of state-vectors into their constituent eigen- and principal vectors is first developed in the context of the 10-cell structure shown in Fig. 1, but loaded at the free-end only and with no intermediate support, for which one has

$$\mathbf{s}(10) = \mathbf{G}^{10}\mathbf{s}(0). \tag{18}$$

The state-vectors $\mathbf{s}(0)$ and $\mathbf{s}(10)$ can be expressed as the linear combinations

$$\mathbf{s}(0) = C_{1,\,0}\mathbf{X}_1 + C_{2,\,0}\mathbf{X}_2 + \cdots C_{12,\,0}\mathbf{X}_{12} = \mathbf{TC}_0 \tag{19}$$

$$\mathbf{s}(10) = C_{1,10}\mathbf{X}_1 + C_{2,10}\mathbf{X}_2 + \cdots C_{12,10}\mathbf{X}_{12} = \mathbf{TC}_{10} \tag{20}$$

where $\mathbf{T}$ is the transformation matrix of eigen- and principal vectors and $\mathbf{C}$ is the column vector of participation coefficients C. The matrix $\mathbf{T}$ transforms $\mathbf{G}$ to its Jordan canonical form $\mathbf{J}$ according to $\mathbf{T}^{-1}\mathbf{GT} = \mathbf{J}$, or $\mathbf{G} = \mathbf{TJT}^{-1}$; powers of $\mathbf{G}$ are then $\mathbf{G}^n = \mathbf{TJ}^n\mathbf{T}^{-1}$. Substituting into Eq. (18) gives $\mathbf{TC}_{10} = \mathbf{TJ}^{10}\mathbf{T}^{-1}\mathbf{TC}_0$, and pre-multiplying by $\mathbf{T}^{-1}$ gives

$$\mathbf{C}_{10} = \mathbf{J}^{10}\mathbf{C}_0; \tag{21}$$

compared with Eq. (18), this surely represents the simplest possible description of spatial evolution as one moves from one end of the structure to the other. In order to apply Eq. (21), one must first determine the vector $\mathbf{C}_0$: the expression $\mathbf{s}(0) = \mathbf{TC}_0$ may be written in partitioned form as

$$\begin{bmatrix}\mathbf{d}(0)\\ \mathbf{F}(0)\end{bmatrix} = \begin{bmatrix}\mathbf{T}_1 & \mathbf{T}_2\\ \mathbf{T}_3 & \mathbf{T}_4\end{bmatrix}\mathbf{C}_0, \tag{22}$$

and the expression $\mathbf{s}(10) = \mathbf{TC}_{10} = \mathbf{TJ}^{10}\mathbf{C}_0$ as

$$\begin{bmatrix}\mathbf{d}(10)\\ \mathbf{F}(10)\end{bmatrix} = \begin{bmatrix}(\mathbf{TJ}^{10})_1 & (\mathbf{TJ}^{10})_2\\ (\mathbf{TJ}^{10})_3 & (\mathbf{TJ}^{10})_4\end{bmatrix}\mathbf{C}_0. \tag{23}$$

From the first row of (22) and the second of (23) one may now construct

$$\begin{bmatrix}\mathbf{d}(0)\\ \mathbf{F}(10)\end{bmatrix} = \begin{bmatrix}\mathbf{T}_1 & \mathbf{T}_2\\ (\mathbf{TJ}^{10})_3 & (\mathbf{TJ}^{10})_4\end{bmatrix}\mathbf{C}_0, \tag{24}$$

in which the column vector on the left-hand side is now known, and hence

$$\mathbf{C}_0 = \begin{bmatrix}\mathbf{T}_1 & \mathbf{T}_2\\ (\mathbf{TJ}^{10})_3 & (\mathbf{TJ}^{10})_4\end{bmatrix}^{-1}\begin{bmatrix}\mathbf{d}(0)\\ \mathbf{F}(10)\end{bmatrix}. \tag{25}$$

The displacements at the free-end, $\mathbf{d}(10)$, and the reactions at the fixed-end, $\mathbf{F}(0)$, are then calculated from the first row of (23) and the second of (22), respectively. Agreement with a FEA is near perfect as seen in the 1st and 2nd columns of Table 1.

4. Distributed loading

The above formalism is now extended to include the distributed loading shown in Fig. 1; from Eq. (17) one may write

$$\mathbf{s}(10) = \mathbf{G}^{10}\mathbf{s}(0) - (\mathbf{G} + \mathbf{G}^2 + \cdots + \mathbf{G}^9)\begin{bmatrix}\mathbf{0}\\ \mathbf{F}_{\text{ext}}\end{bmatrix}, \tag{26}$$

where $\mathbf{F}_{\text{ext}} = [0 \quad -1000 \quad 0 \quad 0 \quad 0 \quad 0]^{\text{T}}$. An external load state-vector can be written as $\mathbf{s}_{\text{ext}} = [0 \quad 0 \quad 0 \quad 0 \quad 0 \quad 0 \quad \mathbf{F}_{\text{ext}}^{\text{T}}]^{\text{T}}$, and expressed in terms of the eigen- and principal vectors as $\mathbf{s}_{\text{ext}} = \mathbf{TC}_{\text{ext}}$, and hence $\mathbf{C}_{\text{ext}} = \mathbf{T}^{-1}\mathbf{s}_{\text{ext}}$. Following the development in Section 3, Eq. (26) can now be written as

$$\mathbf{C}_{10} = \mathbf{J}^{10}\mathbf{C}_0 - (\mathbf{J} + \mathbf{J}^2 + \cdots + \mathbf{J}^9)\mathbf{C}_{\text{ext}}. \tag{27}$$

In partitioned form, the expression $\mathbf{s}(10) = \mathbf{TC}_{10}$ becomes

$$\begin{bmatrix}\mathbf{d}(10)\\ \mathbf{F}(10)\end{bmatrix} = \begin{bmatrix}(\mathbf{TJ}^{10})_1 & (\mathbf{TJ}^{10})_2\\ (\mathbf{TJ}^{10})_3 & (\mathbf{TJ}^{10})_4\end{bmatrix}\mathbf{C}_0 - \begin{bmatrix}\left(\mathbf{T}\sum_{n=1}^{9}\mathbf{J}^n\right)_1 & \left(\mathbf{T}\sum_{n=1}^{9}\mathbf{J}^n\right)_2\\ \left(\mathbf{T}\sum_{n=1}^{9}\mathbf{J}^n\right)_3 & \left(\mathbf{T}\sum_{n=1}^{9}\mathbf{J}^n\right)_4\end{bmatrix}\mathbf{C}_{\text{ext}}, \tag{28}$$

Table 1
Free-end nodal displacement $\mathbf{d}(10)$, and fixed-end nodal force $\mathbf{F}(0)$ predictions under various loading conditions. TMM denotes transfer matrix method, FEA finite element analysis; differences are shown italic.

	End loading only		Distributed loading		Distributed loading with intermediate support	
	TMM	FEA	TMM	FEA	TMM	FEA
$\mathbf{d}(10)$	1.1808	1.1808	4.5602	4.5602	0.3806*1*	0.38062
	−8.5423	−8.5423	−37.136	−37.136	−1.4536	−1.4536
	−0.0039971	−0.0039971	−0.0350*64*	−0.035066	0.06522*6*	0.065229
	−8.4786	−8.4786	−37.075	−37.075	−1.39*454*	−1.3946
	−1.1648	−1.1648	−4.4838	−4.4838	−0.25340	−0.25340
	−8.4609	−8.4609	−37.05*749*	−37.058	−1.3787	−1.3787
$\mathbf{F}(0)$	5000.*002*	5000	27557	27557	1965.1	1965.1
	587.45	587.45	−4269.7	−4269.7	−747.89	−747.89
	0.0036568	0.0036568	−114.6*8*	−114.67	−115.05	−115.03
	174.90	174.90	−1460.8	−1460.8	−1192.0	−1192.0
	−4999.998	−5000	−27,443	−27,443	−1850.0	−1850.0
	−587.45	−587.45	−4269.6	−4269.6	−748.02	−748.02

and from the second row one has

$$\mathbf{F}(10) + \left[\left(\mathbf{T}\sum_{n=1}^{9} \mathbf{J}^n \right)_3 \quad \left(\mathbf{T}\sum_{n=1}^{9} \mathbf{J}^n \right)_4 \right] \mathbf{C}_{\text{ext}} = \left[(\mathbf{TJ}^{10})_3 \quad (\mathbf{TJ}^{10})_4 \right] \mathbf{C}_0. \tag{29}$$

Combine this with the first row of Eq. (22) to give

$$\begin{bmatrix} \mathbf{d}(0) \\ \mathbf{F}(10) + \left[\left(\mathbf{T}\sum_{n=1}^{9} \mathbf{J}^n \right)_3 \quad \left(\mathbf{T}\sum_{n=1}^{9} \mathbf{J}^n \right)_4 \right] \mathbf{C}_{\text{ext}} \end{bmatrix} = \begin{bmatrix} \mathbf{T}_1 & \mathbf{T}_2 \\ (\mathbf{TJ}^{10})_3 & (\mathbf{TJ}^{10})_4 \end{bmatrix} \mathbf{C}_0, \tag{30}$$

in which the column vector on the left-hand side is known, and hence

$$\mathbf{C}_0 = \begin{bmatrix} \mathbf{T}_1 & \mathbf{T}_2 \\ (\mathbf{TJ}^{10})_3 & (\mathbf{TJ}^{10})_4 \end{bmatrix}^{-1} \begin{bmatrix} \mathbf{d}(0) \\ \mathbf{F}(10) + \left[\left(\mathbf{T}\sum_{n=1}^{9} \mathbf{J}^n \right)_3 \quad \left(\mathbf{T}\sum_{n=1}^{9} \mathbf{J}^n \right)_4 \right] \mathbf{C}_{\text{ext}} \end{bmatrix}. \tag{31}$$

The displacements at the free-end, $\mathbf{d}(10)$, and the reactions at the fixed-end, $\mathbf{F}(0)$, are now calculated from the first row of (28) and the second of (22), respectively. Again, agreement with FEA is near perfect, as seen in the 3rd and 4th two columns of Table 1.

Now consider the effect of a simple-support at the 7th nodal cross-section, as shown in Fig. 1. First define $\mathbf{F}_{\text{ext}}(7) = [0 \quad -1000 \quad 0 \quad 0 \quad 0 \quad F]^{\mathrm{T}}$, where F is the unknown support reaction. For the complete structure one may write

$$\mathbf{s}(10) = \mathbf{G}^{10}\mathbf{s}(0) - (\mathbf{G} + \mathbf{G}^2 + \mathbf{G}^4 + \cdots + \mathbf{G}^9) \begin{bmatrix} \mathbf{0} \\ \mathbf{F}_{\text{ext}} \end{bmatrix} - \mathbf{G}^3 \begin{bmatrix} \mathbf{0} \\ \mathbf{F}_{\text{ext}}(7) \end{bmatrix}, \tag{32}$$

(note the absence of the $\mathbf{G}^3$ term in the summation) or in terms of the participation coefficients

$$\mathbf{C}_{10} = \mathbf{J}^{10}\mathbf{C}_0 - (\mathbf{J} + \mathbf{J}^2 + \mathbf{J}^4 + \cdots + \mathbf{J}^9)\mathbf{C}_{\text{ext}} - \mathbf{J}^3\mathbf{C}_7, \tag{33}$$

where $\mathbf{C}_7 = \mathbf{T}^{-1} \begin{bmatrix} \mathbf{0} \\ \mathbf{F}_{\text{ext}}(7) \end{bmatrix}$. The state-vector $\mathbf{s}(10)$ in partitioned form becomes

$$\begin{bmatrix} \mathbf{d}(10) \\ \mathbf{F}(10) \end{bmatrix} = \begin{bmatrix} (\mathbf{TJ}^{10})_1 & (\mathbf{TJ}^{10})_2 \\ (\mathbf{TJ}^{10})_3 & (\mathbf{TJ}^{10})_4 \end{bmatrix} \mathbf{C}_0 - \begin{bmatrix} \left(\mathbf{T}\sum\limits_{n=1,2,4\cdots}^{9} \mathbf{J}^n \right)_1 & \left(\mathbf{T}\sum\limits_{n=1,2,4\cdots}^{9} \mathbf{J}^n \right)_2 \\ \left(\mathbf{T}\sum\limits_{n=1,2,4\cdots}^{9} \mathbf{J}^n \right)_3 & \left(\mathbf{T}\sum\limits_{n=1,2,4\cdots}^{9} \mathbf{J}^n \right)_4 \end{bmatrix} \mathbf{C}_{\text{ext}} - \begin{bmatrix} (\mathbf{TJ}^3)_1 & (\mathbf{TJ}^3)_2 \\ (\mathbf{TJ}^3)_3 & (\mathbf{TJ}^3)_4 \end{bmatrix} \mathbf{C}_7. \tag{34}$$

From the second row one has

$$\mathbf{F}(10) + \left[\left(\mathbf{T}\sum_{n=1,2,4\cdots}^{9} \mathbf{J}^n \right)_3 \quad \left(\mathbf{T}\sum_{n=1,2,4\cdots}^{9} \mathbf{J}^n \right)_4 \right] \mathbf{C}_{\text{ext}} + \left[(\mathbf{TJ}^3)_3 \quad (\mathbf{TJ}^3)_4 \right] \mathbf{C}_7 = \left[(\mathbf{TJ}^{10}t)_3 \quad (\mathbf{TJ}^{10})_4 \right] \mathbf{C}_0. \tag{35}$$

Combine this with the first row of Eq. (22) to give

$$\begin{bmatrix} \mathbf{d}(0) \\ \mathbf{F}(10) + \left[\left(\mathbf{T}\sum\limits_{n=1,2,4\cdots}^{9} \mathbf{J}^n \right)_3 \quad \left(\mathbf{T}\sum\limits_{n=1,2,4\cdots}^{9} \mathbf{J}^n \right)_4 \right] \mathbf{C}_{\text{ext}} + \left[(\mathbf{TJ}^3)_3 \quad (\mathbf{TJ}^3)_4 \right] \mathbf{C}_7 \end{bmatrix} = \begin{bmatrix} \mathbf{T}_1 & \mathbf{T}_2 \\ (\mathbf{TJ}^{10})_3 & (\mathbf{TJ}^{10})_4 \end{bmatrix} \mathbf{C}_0, \tag{36}$$

and hence

$$\mathbf{C}_0 = \begin{bmatrix} \mathbf{T}_1 & \mathbf{T}_2 \\ (\mathbf{TJ}^{10})_3 & (\mathbf{TJ}^{10})_4 \end{bmatrix}^{-1} \times \begin{bmatrix} \mathbf{d}(0) \\ \mathbf{F}(10) + \left[\left(\mathbf{T}\sum\limits_{n=1,2,4\cdots}^{9} \mathbf{J}^n \right)_3 \quad \left(\mathbf{T}\sum\limits_{n=1,2,4\cdots}^{9} \mathbf{J}^n \right)_4 \right] \mathbf{C}_{\text{ext}} + \left[(\mathbf{TJ}^3)_3 \quad (\mathbf{TJ}^3)_4 \right] \mathbf{C}_7 \end{bmatrix}. \tag{37}$$

The state-vector at the support is then

$$\mathbf{s}(7) = \mathbf{TJ}^7\mathbf{C}_0 - \mathbf{T}(\mathbf{J} + \mathbf{J}^2 + \cdots \mathbf{J}^6)\mathbf{C}_{\text{ext}}; \tag{38}$$

the y-component of the displacement at the support is calculated as $31.8F - 232527$, and for this to be equal to zero requires $F = 7312.1$ N. With F now known, the displacements at the free-end $\mathbf{d}(10)$, and the reactions at the fixed-end $\mathbf{F}(0)$, are calculated from the first row of (34) and the second of (22), respectively. Once again agreement with FEA is near perfect, as seen in the 5th and 6th columns of Table 1.

5. Numerical consideration and limitations

Transfer matrix methods have acquired a reputation for numerical inaccuracy, which is not unfounded: early applications to vibration problems, employing Holzer techniques, were susceptible to multiple round-off errors, consistent with the rudimentary computing facilities of the time. For more recent problems of the present type, it has been noted (Zhong and Williams, 1995) that construction of a transfer matrix through the inversion of a partition of the stiffness matrix of a single cell, as described in the Introduction, can lead to ill-conditioning. This arises because a typical element of the stiffness matrix of a pin-jointed structure is proportional to EA/l, and Young's modulus is large, here $E = 200 \times 10^3$ N/mm^2; in turn, inversion leads to ill-conditioning with the transfer matrix $\mathbf{G}$ having a condition number of the order 10^{12}. However, this problem is easily remedied by setting $E = 2$ N/mm^2 with displacement predictions scaled accordingly; so modified, the condition number of $\mathbf{G}$ reduces to 731.

Ill-conditioning in the present problem arises when one employs powers of the Jordan canonical form – the largest eigenvalue of the transfer matrix is $\lambda_1 = 16.78$, and the smallest is its inverse. Each of the examples considered above requires inversion of the matrix $\begin{bmatrix} \mathbf{T}_1 & \mathbf{T}_2 \\ (\mathbf{TJ}^{10})_3 & (\mathbf{TJ}^{10})_4 \end{bmatrix}$, which has a condition number of the order 10^{13} (16.78^{10} is of the order 10^{12}); thus while the results presented in Table 1 are in near perfect agreement, they do not show other errors that accumulate. For example, in calculating the displacement vector at the free-end, $\mathbf{d}(10)$ in terms of the participation factors, one also calculates the force vector $\mathbf{F}(10)$, as this pair constitute the state-vector $\mathbf{s}(10)$. For the case of loading at the free-end only, this is calculated perfectly as $\mathbf{F}(10) = [0 \quad -1000 \quad 0 \quad 0 \quad 0 \quad 0]^{\mathrm{T}}$, indicating that ill-conditioning to this degree is not in itself a source of error; this is because the vector $[\mathbf{d}(0)^{\mathrm{T}} \quad \mathbf{F}(10)^{\mathrm{T}}]^{\mathrm{T}}$ is known exactly, the only possible error being the inability of the computer to represent it precisely.

In contrast, when loading is distributed one finds $\mathbf{F}(10) = [-0.034 \quad -1000.003 \quad 0.004 \quad 0.007 \quad 0.019 \quad 0.011]^{\mathrm{T}}$, and when the support is added, $\mathbf{F}(10) = [-0.024 \quad -1000 \quad 0.008 \quad -0.0045 \quad 0.0016 \quad 0.0075]^{\mathrm{T}}$. These errors can be attributed to the ill-conditioning, as noted above, *in conjunction* with round-off errors in the left-hand sides of Eqs. (30) and (36); this is quite consistent with standard descriptions of ill-conditioning (Golub and Van Loan, 1996).

However, more can be gleaned by examining the vector of participation coefficients $\mathbf{C}_0$ for each case. For end loading only, one has

$$\mathbf{C}_0 = [0\ \ 0\ \ 0\ \ 0\ \ 0\ \ -353\ \ 0\ \ 0\ \ 347\ \ 3803\ \ 4500\ \ -500]^{\mathrm{T}}; \tag{39}$$

the first three zeros indicate that the state-vector $\mathbf{s}(0)$ has no contributions from eigenvectors associated with eigenvalues greater than unity (in particular $\lambda_1 = 16.78, \lambda_2 = 3.53$ and $\lambda_3 = -14.24$). One should expect as much, since these eigenvectors describe self-equilibrating load patterns that decay (in the sense of Saint-Venant's principle) as one moves from *right*-to-*left*. The next two zeros pertain to the eigenvalues $\lambda_4 = \lambda_1^{-1} = 0.0596$ and $\lambda_5 = \lambda_2^{-1} = 0.2829$, indicating that $\mathbf{s}(0)$ has no contributions from these two self-equilibrating eigenvectors which decay as one moves from *left*-to-*right*. The term $C_{6,0} = -353$ is associated with an eigenvector describing self-equilibrating force which is consistent with the suppression of Poisson's ratio contraction at the fully fixed left-hand end, with eigenvalue $\lambda_6 = \lambda_3^{-1} = -0.0702$ as one moves from *left*-to-*right*. The final two zeros indicate that $\mathbf{s}(0)$ has no contributions from the eigenvector describing rigid-body displacement in the *x*-direction, or the coupled principal vector describing a tensile force.

In contrast, for the case of distributed loading one has

$$\begin{aligned}\mathbf{C}_0 = [&-8.41\quad 37.08\quad 8.70\quad -8.40\quad 37.07\quad -1932\\ &-0.02\quad -0.004\quad 1906\quad 26988\quad 22500\quad -5000]^{\mathrm{T}}.\end{aligned} \tag{40}$$

The 7th and 8th terms indicate that contributions from the rigid-body displacement and tensile force are both very small, and should probably be zero; these terms most likely represent accumulated errors from the sum of powers of the Jordan canonical form, as in Eq. (31). Also the term $C_{6,0} = -1932$ is again the largest contributor of self-equilibrated loading. These features are common with the vector in Eq. (39). However, one now has near equal contributions from *left*-to-*right* and their reciprocal *right*-to-*left* eigenvectors, for example the coefficients 37.07 and 37.08, respectively, and -8.40 and -8.41. While these coefficients may well be small compared with the 10th and 11th, the first three terms pertain to eigenvalues that are greater than unity, so their effect increases as one moves from *left*-to-*right*. For the largest eigenvalue $\lambda_1 = 16.78$, the coefficient -8.41 will increase by a factor of the order 10^{12} over ten cells. Thus ill-conditioning can be viewed first, as the source of errors in the vector $\mathbf{C}_0$ and second, the means by which these errors are magnified – metaphorically, a case of Saint-Venant's principle acting in reverse.

The above suggests that the present theory, at least in its current stage of development, is limited in its accuracy if the number of repeating cells becomes large. Indeed, if one increases the number of cells to 50, one must calculate $\mathbf{J}^{50}$ for which the condition number is of the order of 10^{61}; the simplest case of end loading only is then hopelessly inaccurate. On the other hand, one can employ equivalent continuum properties derived from the eigen- and principal vectors of a single cell (Stephen and Wang, 1996) to good effect: the deflection under the load applied at the free-end according to a Timoshenko beam model (Reismann and Pawlik, 1980) is then

$$v = -\frac{1000 \times 50^3}{3EI}\left(1 + \frac{3EI}{\kappa AG \times 50^2}\right), \tag{41}$$

and one find $v = 981.43$ mm which is just 0.07% greater than the averaged nodal displacement predictions from FEA.

6. Conclusions

A repetitive pin-jointed structure subject to point-wise distributed loading, with and without an intermediate support, has been analysed using a transfer matrix procedure. The state-vectors are expressed in terms of a column vector of participation coefficients of the eigen- and principal vectors, and spatial evolution as one moves along the structure is then expressed in terms of powers of the Jordan canonical form. This formulation provides an insight into the nature and effects of ill-conditioning.

References

Golub, G.H., Van Loan, C.F., 1996. Matrix Computations, third ed. The John Hopkins University Press, Baltimore (See section 2.7).

Langley, R.S., 1996. A transfer matrix analysis of the energetics of structural wave motion and harmonic vibration. Proceedings of the Royal Society, Series A, Mathematical, Physical and Engineering Sciences 452 (1950), 1631–1648.

Reismann, H., Pawlik, P.S., 1980. Elasticity Theory and Applications. Wiley, Chichester. pp. 221–222.

Stephen, N.G., 2006. Transfer matrix analysis of the elastostatics of one-dimensional repetitive structures. Proceedings of the Royal Society, Series A, Mathematical, Physical and Engineering Sciences 462 (2072), 2245–2270.

Stephen, N.G., Ghosh, S., 2005. Eigenanalysis and continuum modelling of a curved repetitive beam-like structure. International Journal of Mechanical Sciences 47 (12), 1854–1873.

Stephen, N.G., Wang, P.J., 1996. On Saint-Venant's principle in pin-jointed frameworks. International Journal of Solids and Structures 33 (1), 79–97.

Stephen, N.G., Zhang, Y., 2006. Eigenanalysis and continuum modelling of pre-twisted repetitive beam-like structures. International Journal of Solids and Structures 43 (13), 3832–3855.

Zhong, W.X., Williams, F.W., 1995. On the direct solution of wave propagation for repetitive structures. Journal of Sound and Vibration 181 (3), 485–501.